Journal of KSNVE, Vol. 8, No. 4, pp. 733~740, 1998.

〈Orignal Paper〉

Narrowband Noise Attenuation Characteristics of In-Duct Acoustic Screens

덕트 내 음향 스크린의 협대역 소음 저감 특성

Minhong Rim* and Yang-Hann Kim**
임 민 홍·김 양 한

(Received February 20, 1998 ; Accepted June 17, 1998)

Key Words : Acoustic Screen(음향 스크린), Sound Paths Asymmetry(음파 경로 비대칭성), Narrowband Noise Attenuation(협대역 소음 저감), Transmission Loss(투과 손실)

ABSTRACT

Noise attenuation characteristics of in-duct acoustic screens are studied. Transmission loss was measured for various acoustic screens with different geometry. It was observed that sound path asymmetry - which arises when an acoustic screen is installed so as to divide the original duct into two asymmetric channels and recombine - gives rise to large narrowband sound attenuation. Particular attention was paid to understanding the narrowband sound attenuation mechanism. Based on the physical insight gained from the experimental and numerical investigations, an analytical model which accurately describes the narrowband noise attenuation was developed.

요 약

본 논문은 덕트 내에 설치된 음향 스크린의 특성을 연구하였다. 다양한 형상의 음향 스크린의 투과 손실 측정을 통하여, 음향 스크린에 의해 생긴 두 개의 비대칭 경로가 특정 주파수에서 큰 협대역 소음 저감을 발생시킴을 알 수 있었다. 그리고, 실험과 수치적 모의 실험을 바탕으로 이러한 현상을 정확하게 설명할 수 있는 해석적 모델을 개발하였다.

1. Introduction

Rectangular ducts are widely used in ventilation systems. The noise emission problem from these systems has recently received a lot of attention as the demand for quieter environment has increased. Commonly used means of noise control in ducts are the Helmholtz resonators and lined expansion chambers, but these devices have inherent disadvantages of taking up excessive space which makes them inappropriate for installation where strict spatial restriction is imposed. This limitation naturally leads one to consider an in-duct acoustic screen that can serve as a reactive noise control device. Cabelli[1] studied the

* 한국과학기술원 기계공학과 석사과정
** 정회원, 한국과학기술원 기계공학과

effect of placing a turning vane in a curved section of a duct which resulted in a significant attenuation of the sound. Fuller and Bies[2] did a theoretical analysis on turning vanes, but the effect of placing a screen in a straight section of a duct does not seem to be available in literature.

In this paper, the reactive noise attenuation characteristics of the in-duct acoustic screens are studied. Through extensive experiments on the noise reduction performances of various screens with different shape and geometrical orientation in the duct, a very interesting phenomenon was observed. It was found that when an acoustic screen is installed so as to divide the original duct cross-section into two asymmetric paths, large narrowband sound attenuation is attained. The main objective of this paper is the development of an analytical model which accurately describes the physical phenomena involved in the narrowband noise attenuation.

2. Measurement of Transmission Loss

The transmitted noise attenuation performance of an acoustic screen can be assessed quantitatively by the measurement of transmission loss due to its installation in a duct. The experimental set-up is shown in Fig. 1. The details of set-up is described in a reference[3].

As a preliminary experiment, the transmission loss for screens with very simple geometry was measured. Once the screen shape is fixed, there are three geometrical variables that determine the size of the screen and its position in the duct. They are the length L, height h ,and elevation from the bottom of the duct y as shown in Fig. 2. The height of the screen h was fixed at 5 cm in all cases.

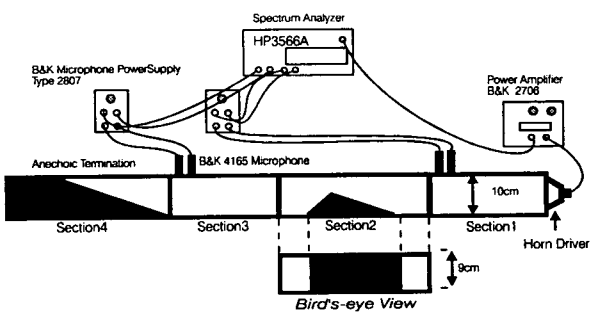

Fig. 1 A sketch of the experimental set-up

It was observed that when an acoustic screen is placed so as to divide the original duct into two asymmetric paths so that the incident wave is divided into two and recombine, a sharp peak results in the TL plot. Figure 3 shows transmission loss for a wedge shaped screen with the length L = 8.7 cm.

Note that totally different noise attenuation characteristics are observed for the case in which $y=0$ cm and the cases in which $y\neq0$. Note that sharp peaks are observed in the TL plot for the $y\neq0$ cases, whereas such behavior does not occur for the case in which $y=0$. This means that the noise attenuation perfor-

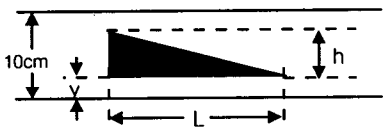

Fig. 2 Important geometrical variables

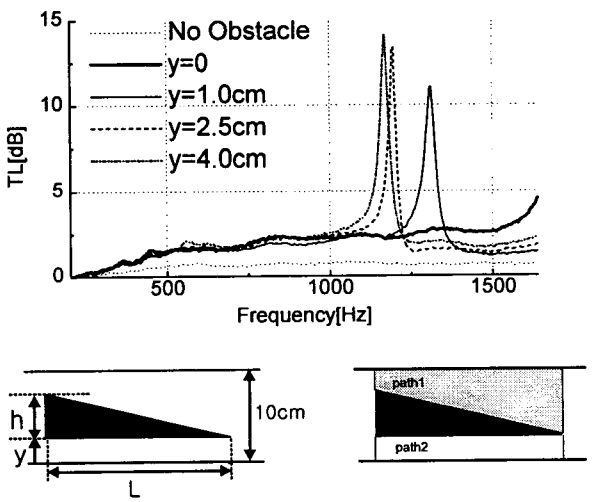

(a) y varied with L=8.7cm, (b) Sound paths asymmetry h=5cm

Fig. 3 The effect of screen location on TL

mance of an acoustic screen depends not only on its shape, but more significantly on the geometrical orientation of the screen installation in the duct. For the case in which $y=0$, the noise attenuation is solely due to the change in the area of the duct which results in broadband reflection of the incident acoustic power. But, the noise attenuation characteristics of the cases in which $y\neq0$ show narrowband noise attenuation in addition to the broadband reflection resulting from the area change.

Figure 4 shows additional experimental results for the cases in which sound paths asymmetry exist. Note that narrowband noise attenuation occur in all cases.

From the foregoing observations, it seems that a strong correlation exists between the sound paths asymmetry and the occurrence of the narrowband sound attenuation, but the generality of such behavior is yet to be tested. Thus, a logical next step would be to check if similar acoustical behavior would occur if theres a perfect symmetry between the two divided paths. Since it is difficult to implement a perfectly symmetric case experimentally, numerical method is used to investigate the effect of perfectly symmetric paths division on TL.

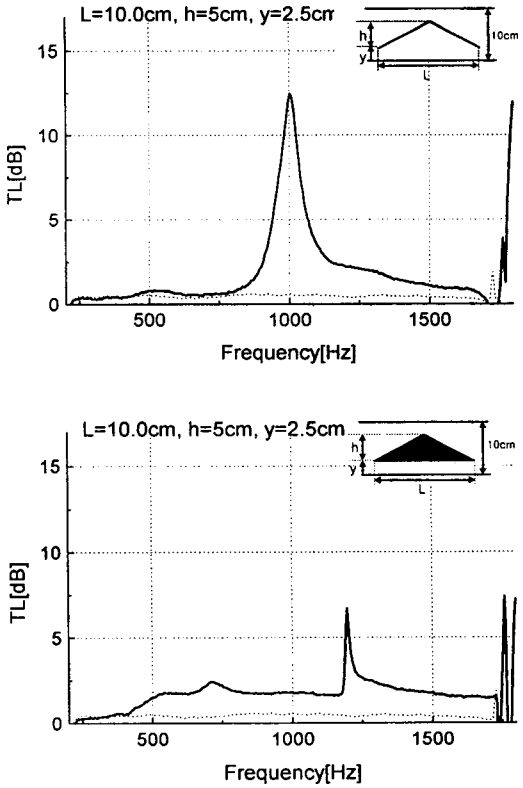

Fig. 4 Transmission loss for various acoustic screens

3. Numerical Simulation

In order to investigate the effect of perfect sound paths symmetry on transmission loss, the TL of a rectangular acoustic screen was calculated numerically.

A widely used commercial package SYSNOISE* was used for the computations. Boundary Element Method(BEM) was used. To simulate the physical situations implemented in the experiments, a 2-dimensional model was used and the boundary conditions were imposed as shown in Fig. 5.

The transmission loss for a rigid rectangular screen with a length of 30 cm and height h of 5 cm was simulated. The simulation was carried out for the perfectly symmetric case ($y=2.5$ cm) and the second one for an asymmetric case ($y=1.0$ cm). In the Fig. 5, one can picture in mind that with $h=5$ cm the two divided channels would be identical when $y=2.5$ cm, whereas they would be asymmetric when $y=1$ cm.

In Fig. 6, the TL for the asymmetric case shows sharp narrowband noise attenuation in

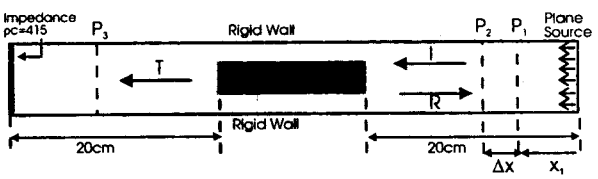

Fig. 5 2D Numerical model for simulation

* SYSNOISE Rev 5.3 LMS Numerical Technologies

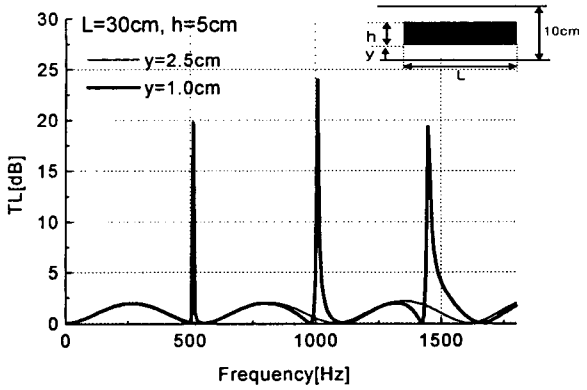

Fig. 6 The effect of sound paths asymmetry on TL

addition to the periodic reflection of sound power due to the simple change in cross-sectional area. But, the perfectly symmetric case only shows periodic reflection of the incident sound power just like a simple expansion chamber. The foregoing results prove that the narrowband noise attenuation is directly associated with the sound paths asymmetry. At this point, we can only guess that the reason for such narrowband sound attenuation might be due to the nonuniform impedance distribution at the discontinuities which could trigger evanescent modes. In order to prove this hypothesis, the paths-asymmetry-induced scattered sound field is visualized experimentally in the following section

4. Measurement of Scattered Sound Field

Section 2 shown in Fig. 1 was replaced with

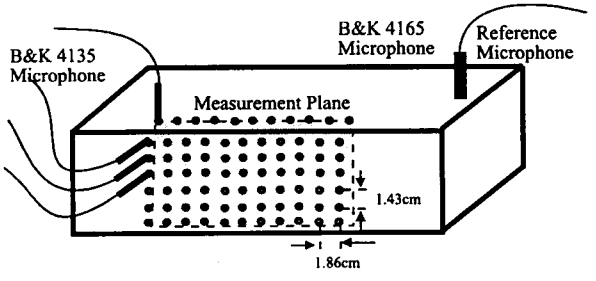

Fig. 7 A sketch of experimental set-up for the measurement of scattered sound field

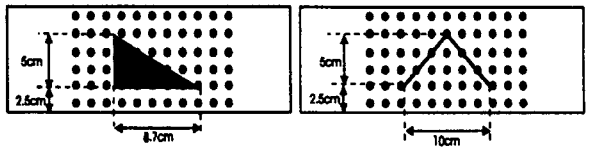

Fig. 8 Geometrical arrangements of the screens for the measurement of scattered sound fields

a new segment of duct with perforations as shown in Fig. 7. Total of 88 holes were perforated with the horizontal spacing of 1.86 cm and the vertical spacing of 1.43 cm. A reference microphone was placed as shown in Fig. 7 and four microphones were used to measure the sound pressure. The step-by-step scanning technique was used to simulate a simultaneous meusurement. The experiment was carried out for the two cases shown in Fig. 8.

The pressure plots at the maximum transmission loss frequencies were obtained for the acoustic screens shown in Fig. 8. The TL plots for these screens are shown in Fig. 3(y = 2.5 cm case) and 4. In Fig. 9(a), it can be seen that the pressure in two asymmetric paths in both cases are 180° out of phase, and transversal phase variation is observed at the discontinuities which is an indication of the higher order mode generation. Especially, the 1st cross mode seems to be dominant in the very vicinity of the discontinuities. The higher order modes in this case dominate over the plane mode as is evident in the scattered sound fields. Resonant behavior is observed in the magnitude plots Fig. 9(b). One can see that out-of-phase acoustic modes are formed in two asymmetric paths in both cases. From this information, we can infer that the first cross mode is directly responsible for forming the standing modes in two asymmetric paths whose phases differ by 180°.

From the foregoing observation, it can be concluded that higher order mode generation plays an important role in the narrowband noise attenuation phenomenon.

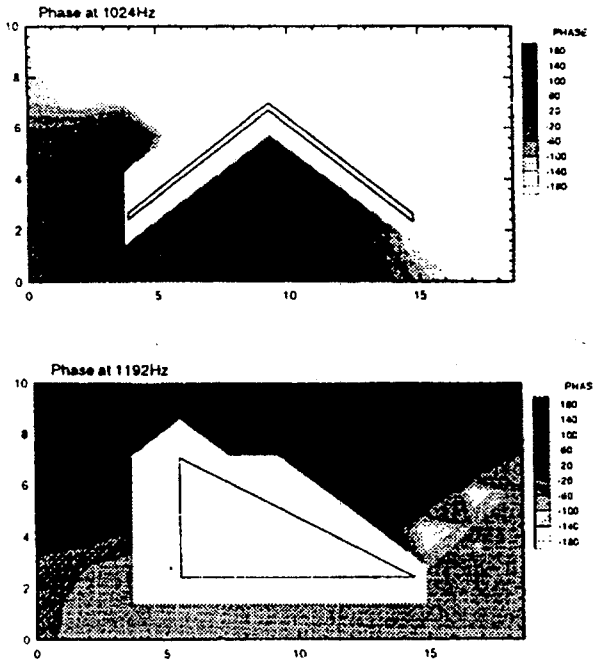

(a) Phase plot

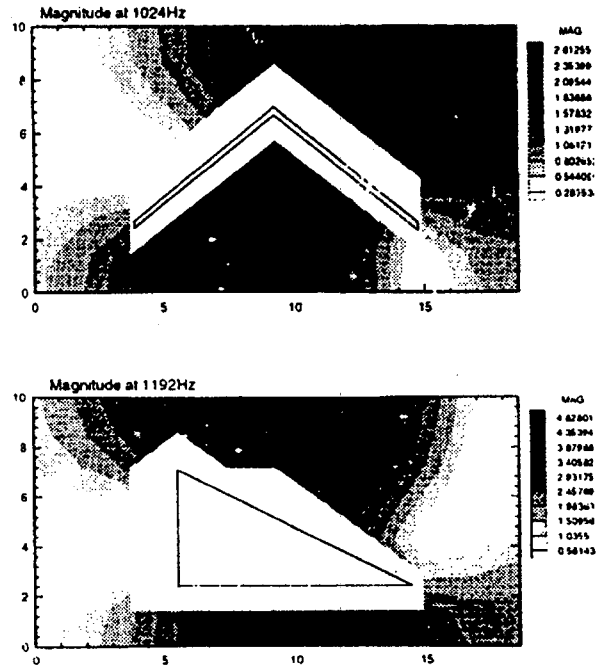

(b) Magnitude plot

Fig. 9 Scattered sound field at peak TL frequency

5. Analytical Model

5.1 Analytical Model for Wedge-shaped Screen

The wave propagation in the duct system with a wedge-shaped screen installed can be analyzed by dividing it into four sections as shown in Fig. 10. Careful observation of the scattered sound fields at the maximum TL frequencies in Fig. 9 informs us that the transversal phase and magnitude variations within Path 1 and Path 2 are negligible, and therefore assuming plane wave propagation in the two divided paths seems reasonable. At each discontinuity an infinite set of higher order modes are generated. Since the frequency range of interest is confined to the plane wave region, only the plane wave modes will propagate without attenuation, but the contribution of the higher order modes near the discontinuities is significant at the peak TL frequency as is evident in Fig. 9; hence considered in the transmitted wave T and reflected wave R.

The mathematical expression in each section is as follows.

$$I = \hat{P}_0^I \exp[i(\omega t - k_0 x)] \tag{1}$$

$$R = \sum_{m=0}^{n} \hat{P}_m^R \cos\left(m\pi \frac{y}{H}\right) \exp[i(\omega t + k_m x)] \tag{2}$$

$$X_1(x,t) = \left\{\hat{C}_1 J_0\left[k_0\left(\frac{W_1 L}{h} - x\right)\right] + \hat{C}_2 Y_0\left[k_0\left(\frac{W_1 L}{h} - x\right)\right]\right\} \times \exp(i\omega t) \tag{3}$$

$$I_2 = \hat{I}_2 \exp[i(\omega t - k_0 x)] \tag{4}$$

$$R_2 = \hat{R}_2 \exp[i(\omega t + k_0 x)] \tag{5}$$

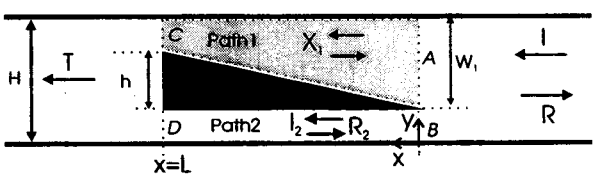

Fig. 10 Definition sketch for theoretical analysis of the wedge-shaped screen

$$T = \sum_{m=0}^{n} \hat{P}_m^T \cos\left(m\pi \frac{y}{H}\right) \exp[i(\omega t - k_m x)] \qquad (6)$$

,where $k_m = k_x = \sqrt{(\omega/c)^2 - (m\pi/H)^2}$ and X_1 describes the sound field in Path1(see Fig. 10). is obtained from the Webster Horn equation[4].

Pressure at the junctions A, B, C, and D were matched so that the mean pressure across each junction is equalized. Velocity was also matched at $x=0$ and $x=L$. Based on the scattered sound fields obtained for the maximum TL frequencies, the number of higher modes to be considered was set equal to two ($n=2$) so that two nonpropagating higher modes are taken into account in addition to the plane mode in the reflected wave R and the transmitted wave T. With $n=2$, one would then deal with 10 equations and 11 unknown coefficients. Setting $\hat{P}_0^I = 1+0i$ as a reference value, all the other coefficients can be found. Based on the same assumptions and physical reasoning in this section, theoretical analysis was also performed for the rectangular screen.

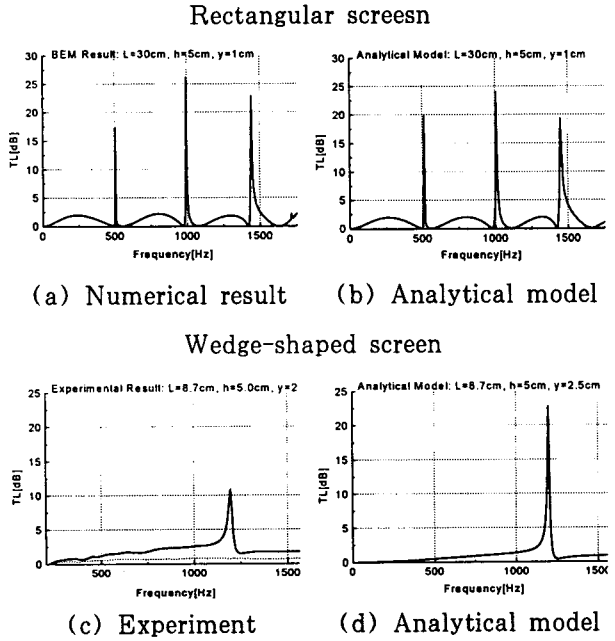

Fig. 11 Validity of analytical model

5.2 Validation of Analytical Results

The validity of the analytical model was confirmed by comparing the analytical results with those of the numerical method and experiments. Figure 11 shows the comparisons. The analytical result for the rectangular screen with $L=30$ cm, $h=5$ cm, $y=1$ cm - see Fig. 11(a) and (b) - shows close-to-perfect agreement with the numerical result.

The comparison between the analytical and the experimental results in Fig. 11 confirms that the analytical model is reliable. Figure 11(c) and (d) shows the comparison between the experimental and analytical results for the wedge-shaped screen with $L=8.7$ cm, $h=5$ cm, $y=2.5$ cm. Note that the peak TL frequency is precisely predicted, but the magnitude of the peak TL in the analytical model are overes- timated and its bandwidth is slightly narrower than that of the experimental result, due to the neglect of damping effect.

6. Understanding Narrowband Sound Attenuation Mechanism

The contribution of the evanescent modes at the discontinuities is obtained. Fig. 12 shows the contribution of the first cross mode normalized by the incident wave coefficient $\hat{P}_0^I$ at the inlet and outlet interface for the rectangular screen: $\hat{P}_1^R / \hat{P}_0^I$ and $\hat{P}_1^T / \hat{P}_0^I$ respectively. Note that the contribution of the 1st cross mode is significant at the frequencies where TL peaks, but is almost negligible at other frequencies. It is important to note that the 1st higher order mode contribution is zero in the perfectly symmetric case shown in Fig. 12(d) and (f). As a result, spiky noise attenuation is not observed in Fig. 12(b). From these data, we can infer that the asymmetric transversal impedance distribution at the discontinuities is responsible for the

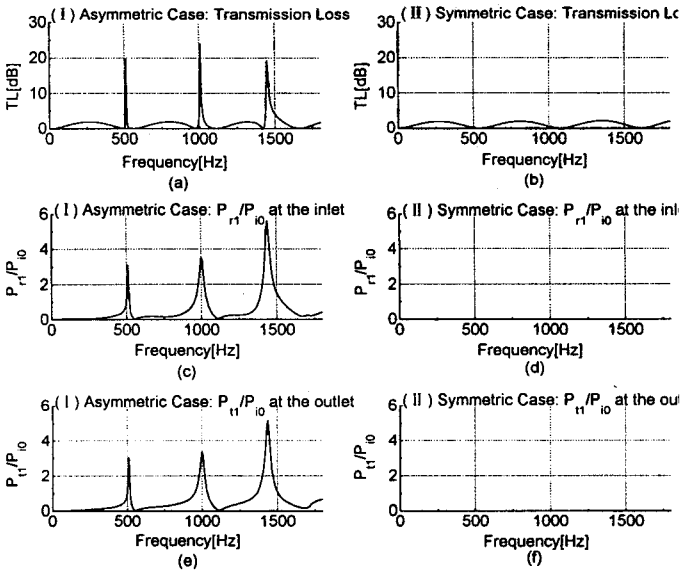

Fig. 12 Contribution of 1st higher order mode

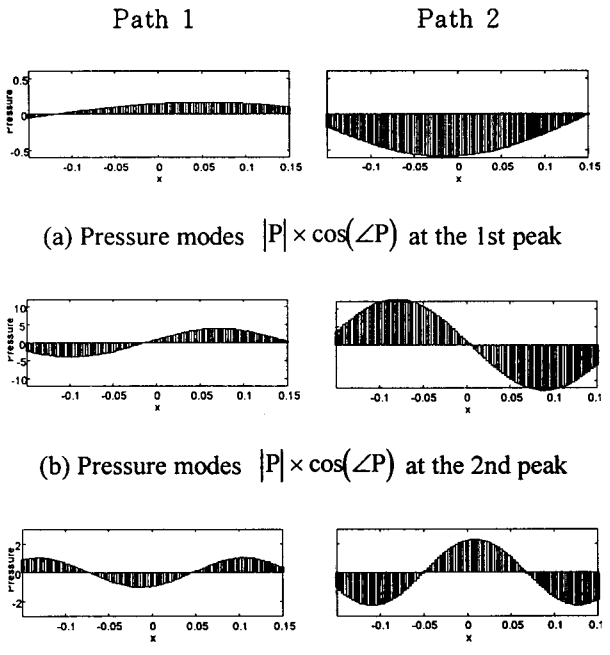

(a) Pressure modes $|P| \times \cos(\angle P)$ at the 1st peak

(b) Pressure modes $|P| \times \cos(\angle P)$ at the 2nd peak

(c) Pressure modes $|P| \times \cos(\angle P)$ at the 3rd peak

Fig. 13 Theoretically obtained acoustic modes at peak TL frequencies for the rectangular screen of $L = 30$ cm, $h = 5$ cm. $y = 1$ cm. designates the acoustic pressure. The x axis is in meters

excitation of the 1st cross mode.

A close scrutiny on the previously obtained results reveals an interesting behavior. Looking carefully at Fig. 6 again, it can be noticed that the locations of the three sharp peaks in the TL plot for the asymmetric case are almost identical to the locations of the troughs in the TL plot for the symmetric case, which correspond to $L = n\lambda/2$, where L is the screen length, λ is the wave lenght and n an integer. The locations of the first two peaks coincide with those of the first two troughs. The third peak shows a slight deviation from the third trough. This is because of the added mass effect induced by the evanescent modes in the very vicinity of the discontinuities. Nevertheless a correspondence does seem to exist between the third peak and trough. In order to see if theres a definite relationship between the screen length and the wavelengths corresponding to the peak TL frequencies, the pressure distributions along the two asymmetric paths were obtained at each peak TL frequency for the rectangular screen of $L = 30$ cm, $h = 5$ cm, $y = 1$ cm(See Fig. 6 for the TL plot). Figure 13 shows the theoretically obtained acoustic modes at each peak frequency along Path 1 and Path 2. Path 1 and Path 2 designate the upper and lower path respectively. These results suggest that the first peak corresponds to the frequency at which $L_{eff} = \lambda/2$ and the second peak at which $L_{eff} = \lambda$ and so on. To put it in general terms, the nth peak corresponds to where $L_{eff} = n\lambda/2$. Here L_{eff} designates the effective screen length, perceived by the air particles which is usually longer than the actual length due to the added mass effect. It is important to note that the pressure modes in Path 1 and Path 2 are out of phase. This is a clear indication that the 1st cross mode generated at the junctions is directly responsible for the formation of out-of-phase interference fields in

two asymmetric paths.

7. Conclusions

The noise attenuation characteristics of various in-duct acoustic screens was studied. Experimental results showed that when an acoustic screen is installed in the duct so as to form a section with two asymmetric paths, large narrowband sound attenuation occurs. Careful observation of the scattered sound fields obtained experimentally showed that the higher order mode generation, especially the 1st cross mode, is significant at the peak transmission loss frequencies. Therefore an analytical model which takes account of the evanescent mode generation was developed. The analytical model showed very good agreement with the experimental and numerical results. Further investigation on the narrowband sound attenuation mechanism revealed that the frequencies of peak transmission loss are directly related with the length of a screen. It was found that the peak frequencies correspond to the longitudinal resonance frequencies at which the effective length of a screen equals the multiples of one-half wavelength: $L_{eff} = n\lambda / 2$.

The narrowband noise attenuation characteristics of acoustic screens can be applied in situations where tonal noise components are dominant and space limitation is an issue.

References

(1) A. Cabelli, 1980, The Acoustic Characteristics of Duct Bend, Journal of Sound and Vibration, Vol. **68**(3), pp. 369~388.

(2) C.R. Fuller and D.A. Bies, 1978, A Reactive Acoustic Attenuator, Journal of Sound and Vibration, Vol. **56**(1), pp. 45~59.

(3) Minhong Rim, 1998, A Study on Narrowband Noise Reduction Characteristics of Acoustic Screens in a Rectangular Duct, MSc Dissertation, KAIST.

(4) Allan D. Pierce, 1991, Acoustics: An Introduction to Its Physical Principles and Applications, The Acoustical Society of America, pp. 360~362.